Journal of the American College of Cardiology Vol. 54, No. 10, 2009

Published by Elsevier Inc.
ISSN 0735-1097/09/$36.00
doi:10.1016/j.jacc.2009.04.075

Geometry and Degree of Apposition of the CoreValve ReValving System With Multislice Computed Tomography After Implantation in Patients With Aortic Stenosis

Carl J. Schultz, MD, PhD,* Annick Weustink, MD,† Nicolo Piazza, MD,* Amber Otten, MSc,* Nico Mollet, MD, PhD,† Gabriel Krestin, MD, PhD,† Robert J. van Geuns, MD, PhD,* Pim de Feyter, MD, PhD,*† Patrick W. J. Serruys, MD, PhD,* Peter de Jaegere, MD, PhD*

Rotterdam, the Netherlands

Objectives Using multislice computed tomography (MSCT), we sought to evaluate the geometry and apposition of the CoreValve ReValving System (CRS, Medtronic, Luxembourgh, Luxembourgh) in patients with aortic stenosis.

Background There are no data on the durability of percutaneous aortic valve replacement. Geometric factors may affect durability.

Methods Thirty patients had MSCT at a median 1.5 months (interquartile range [IQR] 0 to 7 months) after percutaneous aortic valve replacement. Axial dimensions and apposition of the CRS were evaluated at 4 levels: 1) the ventricular end; 2) the nadir; 3) central coaptation of the CRS leaflets; and 4) commissures. Orthogonal smallest and largest diameters and cross-sectional surface area were measured at each level.

Results The CRS (26-mm: n = 14, 29-mm: n = 16) was implanted at 8.5 mm (IQR 5.2 to 11.0 mm) below the noncoronary sinus. None of the CRS frames reached nominal dimensions. The difference between measured and nominal cross-sectional surface area at the ventricular end was 1.6 cm^2 (IQR 0.9 to 2.6 cm^2) and 0.5 cm^2 (IQR 0.2 to 0.7 cm^2) at central coaptation. At the level of central coaptation the CRS was undersized relative to the native annulus by 24% (IQR 15% to 29%). The difference between the orthogonal smallest and largest diameters (degree of deformation) at the ventricular end was 4.4 mm (IQR 3.3 to 6.4 mm) and it decreased progressively toward the outflow. Incomplete apposition of the CRS frame was present in 62% of patients at the ventricular end and was ubiquitous at the central coaptation and higher.

Conclusions Dual-source MSCT demonstrated incomplete and nonuniform expansion of the CRS frame, but the functionally important mid-segment was well expanded and almost symmetrical. Undersizing and incomplete apposition were seen in the majority of patients. (J Am Coll Cardiol 2009;54:911–8) © 2009 by the American College of Cardiology Foundation

Increasing numbers of percutaneous aortic valve replacement (PAVR) procedures are performed worldwide (1). At present there are no data on long-term valve durability, which may be determined by environmental factors (diabetes, renal insufficiency) and valve geometry (2).

When viewed axially the CoreValve ReValving system (CRS) (Medtronic, Luxembourgh) is round; the outflow of the left ventricle (LVOT) is usually oval (3,4). This difference in geometry may lead to distortion of the valve after implantation. Distortion may also be caused by prosthesis-host mismatch due to inappropriate sizing or incomplete or nonuniform expansion owing to extensive calcifications (5). Distortion of the valve may in turn affect leaflet configuration, which might cause valvular regurgitation (6). In the absence of acute dysfunction, uneven distribution of stress on the leaflets may affect long-term durability (2).

The configuration (diameters and cross-sectional area) and apposition of the CRS were investigated using multislice computed tomography (MSCT) in 30 patients treated for aortic stenosis.

Methods

Patients. The population consisted of 30 patients who underwent CRS implantation for aortic stenosis. MSCT

From the Departments of *Cardiology and †Radiology, Erasmus Medical Center, Rotterdam, the Netherlands.

Manuscript received February 26, 2009; revised manuscript received April 20, 2009; accepted April 26, 2009.

Abbreviations and Acronyms

CRS = CoreValve ReValving System
CSA = cross-sectional surface area
D1 = smallest diameter
D2 = largest diameter
IQR = interquartile range
LVOT = left ventricular outflow tract
MSCT = multislice computed tomography
PAVR = percutaneous aortic valve replacement
TTE = transthoracic echocardiography

was performed after PAVR in all patients, 19 of whom had already had a scan before PAVR. Written informed consent was obtained in all patients (post-marketing surveillance registry). The CRS (Fig. 1) and technique of implantation have previously been described in detail (1).

MSCT protocol. Dual-source computed tomography was performed similar to a coronary protocol described before but without X-ray tube current modulation (100% of dose) (7). Functional computed tomography coronary angiography datasets were reconstructed using a single-segmental reconstruction algorithm: slice thickness, 0.75 mm; increment, 0.4 mm; medium-to-smooth convolution kernel (B26f); and sharp kernel (B46f), resulting in a spatial resolution of 0.6 to 0.7 mm in-plane and 0.4 to 0.5 mm through-plane. The expected radiation dose ranged between 8 and 20 mSv.

Measures of interest on MSCT. With Siemens Circulation software, the 3 perpendicular analysis windows were aligned to obtain 2 longitudinal slices and 1 axial slice through the aortic root (pre-implantation) so that the most caudal attachments of all 3 native aortic leaflets were seen simultaneously in 1 axial image, which was then defined as the native annulus (Fig. 2). At this level the smallest diameter (oblique sagittal view) approximates the parasternal long-axis view on transthoracic echocardiography (TTE); the largest diameter (oblique coronal view) approximates the posteroanterior view on angiography (3).

Measurements of the CRS frame were done on axial images. The 3 perpendicular analysis windows were aligned to obtain 2 longitudinal slices and 1 axial slice through the CRS so that the welding points of the ventricular end appeared simultaneously in an axial image (Fig. 3).

We measured the smallest and largest perpendicular diameters of the native aortic annulus and of the implanted CRS frame at: 1) the ventricular end where the CRS first appeared as a ring in the LVOT; 2) the nadir of the leaflets located 1.5 cells (12 mm) above the ventricular end; 3) central coaptation of the leaflets (3 cells or 24 mm above the ventricular end); and 4) the commissures (4 cells above the ventricular end) (Figs. 1 and 3).

At each axial level the perpendicular smallest (D1) and largest (D2) diameters and cross-sectional surface area (CSA) were measured by connecting the middle of stent struts. Deformation was calculated as the difference between D1 and D2. Axial morphology was defined as noncircular if the ratio of D1/D2 was >10% or circular if it was ≤10%. Apposition was visually assessed. The difference between measured and nominal diameters and CSA was calculated at the ventricular end and central coaptation of the CRS. The variability of diameter measurements (mean [SD]) at the level of central coaptation for D1 was 2% (1.0) or 0.4 mm; for D2 it was 1.8% (1.8) or 0.4 mm; and for CSA it was 2% (1.8) or 0.1 cm^2.

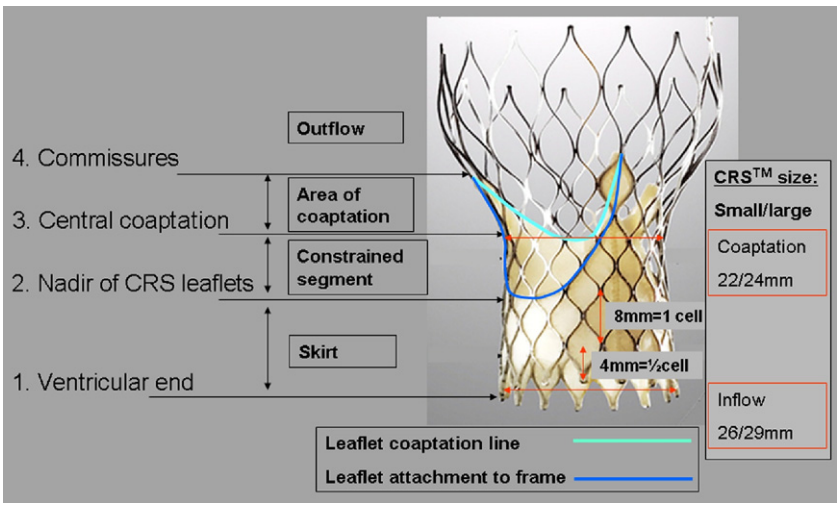

Figure 1 **CRS Structure and Levels of Interest**

The CoreValve ReValving System (CRS) structure and the levels of interest (1, 2, 3, 4) at which dimensions were measured after implantation.

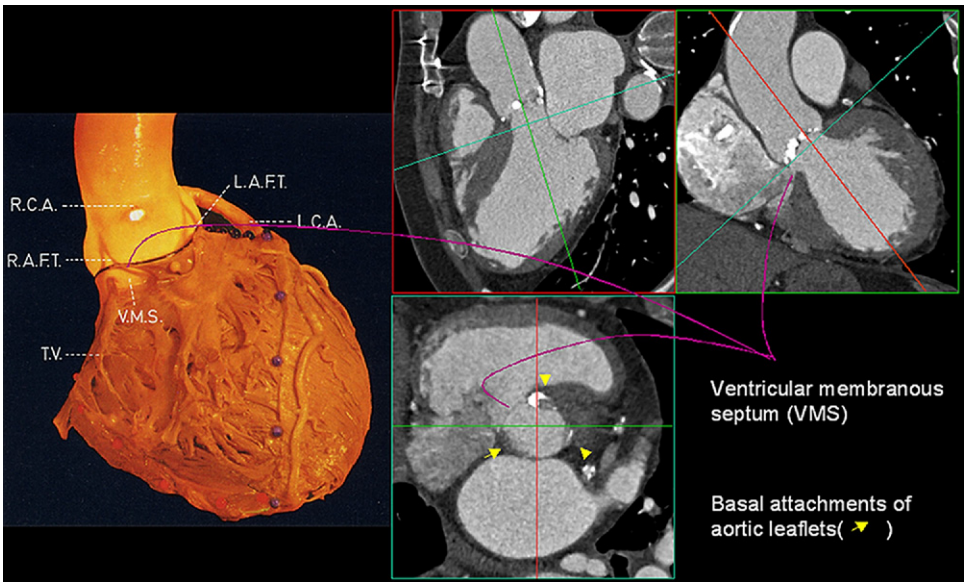

Figure 2 **Native Aortic Root on MSCT**

The axial plane of the native aortic valve on multislice computed tomography (MSCT) and corresponding orientation of an anatomical specimen. The most caudal attachment of all 3 aortic leaflets can be seen in one axial image. The anatomical image is from W.A. Mcalpine. Heart and Coronary Arteries: An Anatomical Atlas for Clinical Diagnosis, Radiological Investigation, and Surgical Treatment. Springer Verlag; October 1974. LAFT = left anterior fibrous trigone; LCA = left coronary artery; RAFT = right anterior fibrous trigone; RCA = right coronary artery; TV = tricuspid valve.

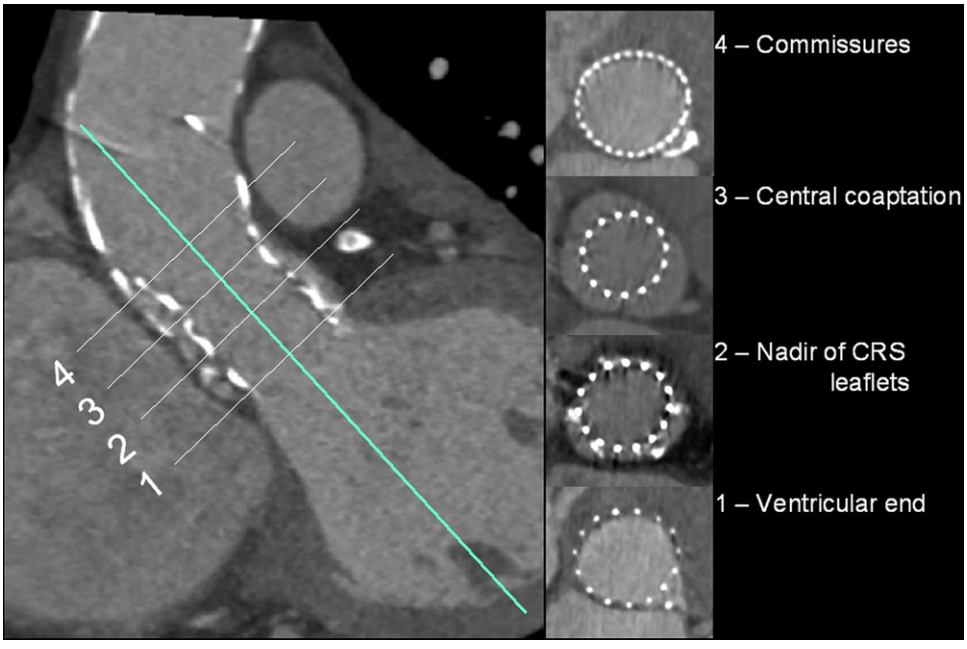

Figure 3 **Levels of Measurement of the CRS on MSCT**

The appearance of the CRS is shown on MSCT (coronal cut plane) after implantation and levels (1, 2, 3, 4) where the dimensions were measured. CRS = CoreValve ReValving System; MSCT = multislice computed tomography.

JACC Vol. 54, No. 10, 2009
September 1, 2009:911–8

Table 1 Clinical Characteristics of the Study Population

Characteristic	MSCT Post-Implant
n, male/female	16/14
Age, yrs	81 (73–84)
Height, cm	166 (160–173)
Weight, kg	73 (63–80)
NYHA functional class	3 (3–3)
Logistic Euroscore	13 (8–16)
Antecedents	
Stroke/transient ischemic attack	5 (17)
Myocardial infarction	5 (17)
Coronary bypass surgery	9 (30)
Percutaneous coronay intervention	8 (27)
Peripheral vascular disease	1 (3)
Comorbidity	
Diabetes	4 (13)
Chronic obstructive pulmonary disease	7 (23)
Serum creatinine, mg/dl	1.08 (0.93–1.46)
Echo Doppler	
Left ventricular function*	
Normal	17 (57)
Moderate	13 (43)
Impaired	0 (0)
Peak transaortic velocity	
Pre-procedure	4.5 (4.0–4.8)
Post-procedure	2.2 (1.7–2.4)
Calcification of aortic root, Agatston score	2,839 (2,024–5,001)
Procedure	
CRS 26	14 (47)
CRS 29	16 (53)
Number CRS implanted	
1 valve	28 (93)
>1 valve	2 (7)
PABV after CRS	5 (17)
Duration between PAVR implant and MSCT, months	1.5 (0–7)

Data are reported as n (%), mean (SD), or median (interquartile range). *Left ventricular function was determined by visual assessment of the baseline transthoracic echocardiogram and classified as normal in case of an estimated ejection fraction of >50%, moderate if 30% to 50%, and poor if <30%.

CRS = CoreValve ReValving System; MSCT = multislice computer tomography; NYHA = New York Heart Association; PABV = percutaneous aortic balloon valvuloplasty; PAVR = percutaneous aortic valve replacement.

The depth of implantation was measured from the ventricular end of the CRS to the floor of the noncoronary sinus (8). The noncoronary sinus was used as a reference point to guide the positioning of the CRS valve under fluoroscopy.

Statistical methods. Variables not normally distributed are given as a median and interquartile range (IQR). Paired data were compared using the Wilcoxon signed rank test. Statistical significance was defined as $p < 0.01$.

Results

Patient characteristics are shown in Table 1. The median depth of implantation was 8.5 mm (IQR 5.2 to 11.2 mm) below the noncoronary sinus. Therefore, coaptation of the CRS leaflets was supra-annular in all patients.

Prosthesis size and expansion. Prosthesis size and expansion is shown in Tables 2 to 5. None of the frames reached the nominal dimensions at either the ventricular end or the central coaptation. The difference in CSA at the ventricular

Table 2 Diameter and Cross-Sectional Area Measured by MSCT at the Ventricular End of the CRS*

	CRS				Native Aortic Root			
Patient #	D1, mm	D2, mm	D2-D1, mm	CSA, cm^2	D1, mm	D2, mm	D2-D1, mm	CSA, cm^2
26-mm inflow valve								
1	17.9	21.3	3.40	2.92	17.6	22.1	4.5	3.18
2	20.0	22.4	2.40	3.40	18.7	20.9	2.2	3.08
3†	15.3	19.2	3.90	2.31	19.2	23.6	4.4	3.64
4	20.8	25.8	5.00	4.19	19.5	24.6	5.1	3.83
5	18.9	26.4	7.50	4.04	19.6	25.3	5.7	4.15
6‡	22.6	26.6	4.00	4.79	20.0	24.9	4.9	3.96
7†	13.9	22.2	8.30	2.56	22.2	27.4	5.2	5.13
8	22.4	24.6	2.20	4.42	22.7	25.5	2.8	4.57
9	23.7	26.1	2.40	4.91	23.9	26.4	2.5	4.98
10	19.3	24.3	5.00	3.52	18.5	23.1	2.0	5.74
11	19.0	23.4	4.40	3.63				
12	18.2	24.6	6.40	3.68				
13	19.2	26.0	6.80	3.70				
14	22.5	26.4	3.90	4.79				
29-mm inflow valve								
15	20.8	25.2	4.40	4.07	19.7	24.3	4.6	3.81
16	21.2	24.9	3.70	3.91	22.2	26.2	4.0	4.61
17‡	24.6	29.0	4.40	5.67	22.3	28.3	6.0	4.95
18§	21.3	30.3	9.00	5.10	22.3	27.9	5.6	4.62
19‡	25.1	29.5	4.40	5.99	22.7	32.5	9.8	5.49
20†	18.1	26.9	8.80	3.91	22.8	24.9	2.1	4.48
21	20.8	24.4	3.60	4.03	25.9	29.1	3.2	5.95
22	25.3	28.3	3.00	5.75	26.1	28.5	2.4	5.86
23	25.4	29.7	4.30	5.85	26.3	28.5	2.2	5.91
24	19.4	25.8	6.40	3.96				
25	18.3	25.2	6.90	3.69				
26	24.3	25.9	1.60	5.27				
27	20.3	23.6	3.30	3.60				
28	25.3	27.4	2.10	5.56				
29	25.7	28.8	3.10	5.75				
30	17.9	26.5	8.60	3.92				
Median (IQR)	20.8 (19.0–23.4)	25.9 (24.5–26.9)	4.4 (3.3–6.4)	4.0 (3.7–5.1)	22.2 (19.6–22.8)	26.2 (24.8–28.1)	4.4 (2.5–5.1)	4.6 (3.9–5.3)

*D1 corresponds with the sagittal (anterior-posterior) diameter and D2 with the coronal (left to right) diameter on MSCT. CSA of a 26-mm inflow valve = 5.3 cm^2, CSA of a 29-mm inflow valve = 6.6 cm^2. †High implant (ventricular end ≤1 mm below the noncoronary sinus, heavily calcified restrictive leaflets). ‡Positioned very low, 12 mm below the noncoronary sinus (ventricular end in section of LVOT that widens into the LV). §Deformation caused by unusually oval annulus.

CSA = cross-sectional surface area; D1 = smallest diameter; D2 = largest diameter; IQR = interquartile range; LV = left ventricular; LVOT = left ventricular outflow tract; other abbreviations as in Table 1.

Table 3 Diameter and Cross-Sectional Area Measured by MSCT at the Level of the Nadir of the CRS Leaflets

Patient #	CRS D1, mm	CRS D2, mm	CRS D2-D1, mm	CRS CSA, cm^2
26-mm inflow valve				
1	20.0	22.3	2.3	3.53
2	20.3	23.0	2.7	3.67
3	17.1	23.5	6.4	3.30
4	21.4	23.1	1.7	3.80
5	18.7	22.1	3.4	3.30
6	19.6	20.9	1.3	3.35
7	17.3	23.7	6.4	3.43
8	21.1	23.8	2.7	4.00
9	21.8	23.7	1.9	4.10
10	20.1	22.8	2.7	3.48
11	19.4	23.4	4.0	3.72
12	19.7	25.1	5.4	3.87
13	19.6	25.1	5.5	3.83
14	20.5	22.8	2.3	3.71
29-mm inflow valve				
15	19.7	22.8	3.1	3.47
16	20.8	23.7	2.9	3.88
17	22.6	24.6	2.0	4.36
18	19.6	26.9	7.3	4.21
19	22.0	25.9	3.9	4.55
20	21.4	26.2	4.8	4.50
21	20.3	23.6	3.3	3.90
22	22.4	24.8	2.4	4.49
23	23.5	24.6	1.1	4.59
24	19.2	24.2	5.0	3.66
25	20.6	26.3	5.7	4.37
26	21.3	25.5	4.2	4.44
27	20.2	25.2	5.0	3.98
28	23.5	25.1	1.6	4.54
29	23.4	24.8	1.4	4.62
30	18.4	26.0	7.6	3.86
Median (IQR)	20.3 (19.6–21.4)	24.0 (23.2–25.1)	3.2 (2.3–5.0)	3.9 (3.7–4.4)

Abbreviations as in Tables 1 and 2.

end was 1.6 cm^2 (IQR 0.9 to 2.6 cm^2), and 0.5 cm^2 (IQR 0.2 to 0.7 cm^2) at the central coaptation.

In 19 patients in whom the native annulus was measured, CRS dimensions conformed to the native annulus dimensions in 11; in 3 patients in whom the CRS was implanted relatively high, there was underexpansion due to calcified native leaflets (Patients #3, #7, and #20). In another 3 patients in whom the CRS was implanted relatively low, the ventricular end was positioned below the annulus in a wider section of the LVOT (Patients #6, #17, and #19).

Patient to prosthesis sizing was estimated by comparing the CSA at the anatomical and functional narrowest point of the CRS (central coaptation) with the CSA of the native annulus. The CRS was anatomically undersized by 24% (IQR 15% to 29%).

Prosthesis deformation. The differences between the D1 and D2 measurements are given in Tables 2 to 5. Symmetrical expansion was seen in only 5 patients and then only at the levels of central coaptation and commissures. The degree of deformation was maximal at the ventricular end (median difference: 4.4 mm [IQR 3.3 to 6.4 mm]), less at the nadir of the CRS leaflets (3.2 mm [IQR 2.3 to 5.0 mm]), and decreased progressively toward the commissures,

Table 4 Diameter and Cross-Sectional Area Measured by MSCT at the Level of the Central Coaptation of the CRS Leaflets*

Patient #	CRS D1, mm	CRS D2, mm	CRS D2-D1, mm	CRS CSA, cm^2	Transthoracic Echo at Time of Follow-Up MSCT Peak Velocity, m/s	Transthoracic Echo at Time of Follow-Up MSCT Estimated Orifice Area, cm^2
26-mm inflow valve						
1	20.8	22.0	1.2	3.62	2.03	1.46
2	20.3	22.7	2.4	3.70	2	2.07
3	19.5	23.0	3.5	3.63	2.1	†
4	20.7	21.3	0.6	3.56	2	1.61
5	19.5	19.6	0.1	3.01	2.4	1.77
6	19.0	20.8	1.8	3.18	2.3	†
7	20.3	22.9	2.6	3.78	2.3	†
8	20.5	21.9	1.4	3.57	2.29	1.10
9	20.0	21.0	1.0	3.45	1.79	1.87
10	21.0	21.7	0.7	3.56	2.30	2.64
11	19.0	22.0	3.0	3.31	1.95	1.12
12	20.2	23.1	2.9	3.70	1.80	1.27
13	20.3	22.2	1.9	3.62	2.01	1.86
14	19.3	22.0	2.7	3.47	1.56	†
29-mm inflow valve						
15	18.6	22.3	3.7	3.26	2.35	†
16	21.0	23.2	2.2	3.87	1.78	†
17	21.3	22.7	1.4	3.73	2.00	1.78
18	19.3	23.5	4.2	3.53	2.16	1.70
19	21.4	23.1	1.7	3.93	1.6	†
20	21.0	25.0	4.0	4.23	2.50	1.42
21	20.8	24.1	3.3	3.92	1.56	1.56
22	23.0	23.6	0.6	4.31	2.45	1.53
23	22.7	23.6	0.9	4.17	2.10	2.27
24	21.3	24.0	2.7	3.97	2.90	1.89
25	20.5	25.3	4.8	4.12	1.50	3.37
26	20.0	23.2	3.2	4.02	2.10	1.58
27	20.5	23.8	3.3	3.80	1.50	1.38
28	22.2	22.3	0.1	3.87	2	1.05
29	20.0	22.1	2.1	3.61	2.5	1.50
30	19.0	23.4	4.4	3.58	1.7	†
Median (IQR)	20.4 (19.6–21)	22.8 (22–23.5)	2.3 (1.3–3.3)	3.7 (3.6–3.9)	2.0 (1.8–2.3)	1.60 (1.43–1.85)

*Nominal diameter at the level of central coaptation of 26- and 29-mm inflow valves are 22 and 24 mm, respectively, and the nominal CSAs are 3.8 and 4.5 cm^2, respectively. †Data not available.
Abbreviations as in Tables 1 and 2.

JACC Vol. 54, No. 10, 2009
September 1, 2009:911–8

Table 5 Diameter and Cross-Sectional Area Measured by MSCT at the Level of the Commissures of the CRS Leaflets

Patient #	CRS D1, mm	CRS D2, mm	CRS D2-D1, mm	CRS CSA, cm^2
26-mm inflow valve				
1	*	*	*	*
2	27.2	28.5	1.3	6.0
3	26.4	26.9	0.5	5.8
4	26.0	26.3	0.3	5.5
5	22.4	24.0	1.6	4.3
6	*	*	*	*
7	26.9	27.8	0.9	6.1
8	24.3	25.7	1.4	4.7
9	26.3	26.8	0.5	5.6
10	26.0	28.1	2.1	5.9
11	25.2	26.1	0.9	5.1
12	26.8	27.9	1.1	5.9
13	26.8	27.3	0.5	5.8
14	22.5	24.4	1.9	4.4
29-mm inflow valve				
15	26.4	28.7	2.3	5.9
16	29.4	30.7	1.3	7.3
17	29.5	30.8	1.3	7.1
18	26.2	27.0	0.8	5.5
19	28.2	29.3	1.1	6.6
20	28.2	30.9	2.7	7.0
21	30.8	31.9	1.1	7.9
22	31.1	31.2	0.1	7.9
23	29.3	30.2	0.9	7.0
24	33.0	33.4	0.4	8.8
25	32.2	34.8	2.6	9.2
26	26.2	28.6	2.4	6.1
27	27.8	28.2	0.4	6.3
28	29.3	29.0	−0.3	6.8
29	25.7	27.8	2.1	5.5
30	26.7	27.6	0.9	5.9
Median (IQR)	26.8 (26.2–29.3)	28.2 (27.0–30.3)	1.1 (0.5–1.7)	6.0 (5.6–7.0)

*Accurate measurements were not possible for technical reasons.
Abbreviations as in Tables 1 and 2.

where it was 1.1 mm (IQR 0.5 to 1.7 mm) (Figs. 4 and 5). Configuration of the CRS in the axial plane at the 4 levels is given in Table 6 and Figures 4 and 6.

Prosthesis apposition. The ventricular end of the CRS was apposed to adjacent tissues in 10 patients, partially apposed (not for >30% of the circumference) in another 16,

Table 6 Axial Shape of the CRS at the Various Levels as Assessed Visually

Shape	Ventricular End	Nadir of Leaflets	Central Coaptation	Commissures
Circular, n	4	10	15	28*
Noncircular, n	26	20	15	0*

Total n = 30 patients. *Could not be assessed in 2 patients.

Table 7 Incomplete Apposition at the Ventricular End of the CRS Was Not Associated With Significant Aortic Regurgitation (>Grade 2 of 4) as Assessed by Transthoracic Echocardiography Immediately Post-Procedure*

		Aortic Regurgitation Post-Procedure ≤1, n	Aortic Regurgitation Post-Procedure ≥2†, n
Incomplete apposition of the CRS at the ventricular end (at least 30° of circumference)	Yes	13	4
	No	5	3

*Apposition of the CRS could not be assessed in 5 patients due to insufficient contrast opacification. Significant aortic regurgitation was paravalvular in all cases. †No patient had aortic regurgitation higher than grade 2.

and could not be assessed in 5. Partial apposition was due to a relatively low implantation in 9 patients and constraining by the calcified leaflets in 6 others with a relatively high implantation (Fig. 4).

At the nadir of the CRS leaflets the frame was well apposed to the compressed native leaflets. At the central coaptation and higher, large sections of the CRS were not apposed to the surrounding tissues. Malapposition at the ventricular end of the CRS was not associated with significant aortic regurgitation on TTE (Table 7).

Discussion

We found that there was incomplete and nonuniform expansion of the frame at all levels. The asymmetry of the ventricular end is explained by conformation of the CRS to the noncircular anatomy of the LVOT (3,4). This is underscored by the observation that in 11 of the 12 patients with both an average depth of implantation and a pre-procedural MSCT, the dimensions of the base of the CRS and the recipient aortic root were similar. The incomplete and nonuniform expansion of the ventricular end may anchor the CRS in the LVOT, thereby facilitating the apposition of the skirt and preventing paravalvar regurgitation (1). The calcified native leaflets may have contributed to the restriction of expansion and anchoring of the CRS, similar to the Edwards-Sapien valve (9).

The middle segment of the CRS, which hosts the leaflets, was less deformed and more apposed at its lower end. This segment is both constrained and highly resistant to external compression in order to preserve the optimal geometry and coaptation of the leaflets. This segment of the CRS was positioned at the narrowest section of the native aortic root (calcified leaflets). This may explain the deformation seen despite the high hoop strength. Zegdi et al. (6) demonstrated, in an acute experiment with a valve of different origin to the CRS and with leaflets residing in the anchoring area of the frame, that deformation of the frame affects the configuration of the leaflets. In the absence of immediate valve dysfunction, the asymmetrical stresses so induced may

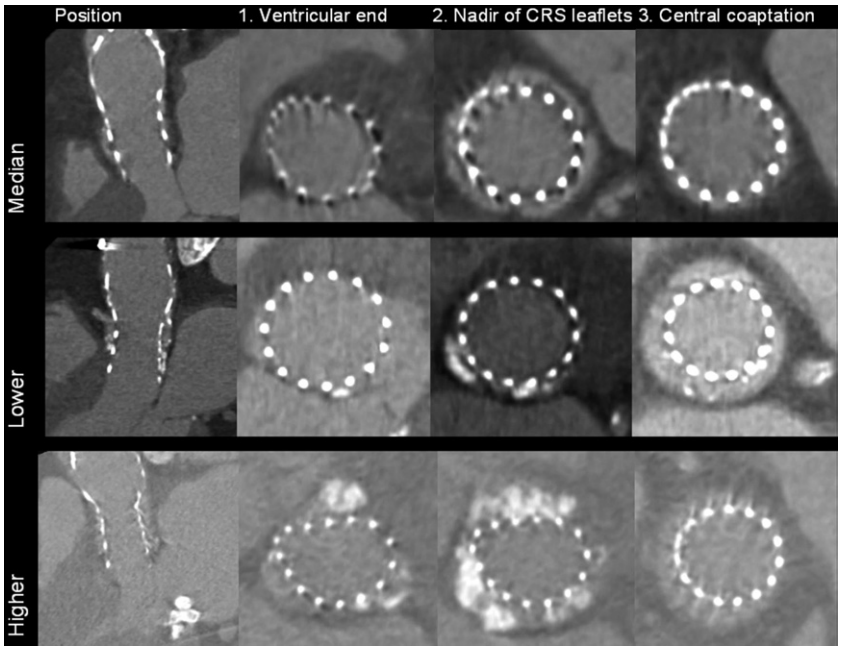

Figure 4 **Axial Morphology of the CRS**

The morphology of the CRS at the levels of interest (1, 2, 3) in 3 patients, where the position within the aortic root was close to the median, lower, or higher. CRS = CoreValve ReValving System.

affect durability (2,6). Whether the deformation observed at the level of the nadir of the CRS leaflets in this study will affect durability requires further study.

Only minimal deformation and underexpansion was seen at the level at which the leaflets coapt. This is explained by the supra-annular position above the calcified native leaflets in combination with the high hoop strength. The midsection is constrained relative to the ventricular end and therefore some anatomical undersizing may be present (on average, by 24% anatomically in this series). The effective orifice area was smaller than the anatomical orifice area in all patients and is clinically more relevant than anatomical or geometric data alone (10,11). The effects of undersizing remain to be evaluated and may be particularly relevant if PAVR is performed in younger patients.

Incomplete apposition of at least 30% of the ventricular end circumference was seen in 61% of patients. Possible explanations are a relatively high or low position within the LVOT and constraining by calcific native leaflets. We did not observe any association between incomplete apposition of the CRS at the ventricular end and aortic regurgitation. It remains to be elucidated whether incomplete apposition is associated with a higher risk of thromboembolism (12).

Study limitations. This study is limited by a small sample of selected patients who underwent MSCT. We observed incomplete and nonuniform expansion of the CRS frame at the ventricular end, in particular. There was some degree of anatomical undersizing due to the unique design of the CRS. Incomplete apposition of struts in the left ventricular outflow and along the length of the CRS was ubiquitous. Further studies to determine long-term effects are required. Yet, detailed assessment of the position and the geometry of the frame in other reports led to a higher implantation strategy to avoid the new left bundle branch block and affect patient management (8,13).

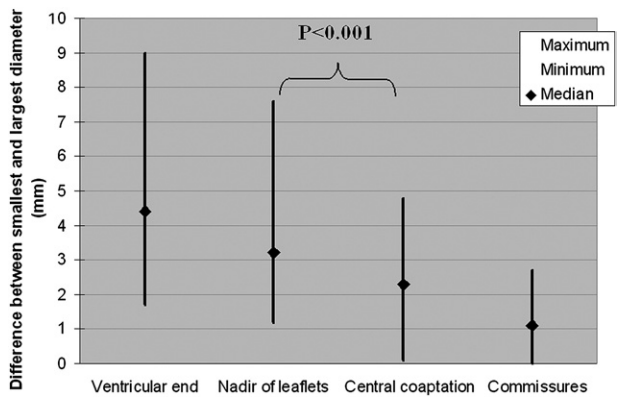

Figure 5 **Degree of Asymmetry at the Various Segments of the CoreValve ReValving System**

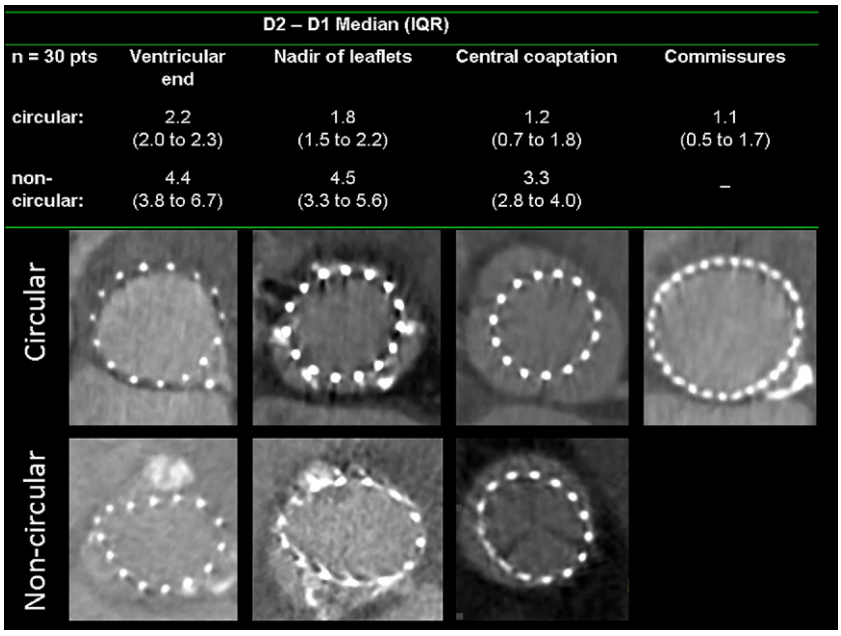

Figure 6 Axial Shape and Dimensions of the CRS at the Various Levels as Assessed Visually

CRS = CoreValve ReValving System; D1 = smallest diameter; D2 = largest diameter; IQR = interquartile range.

Reprint requests and correspondence: Dr. Peter de Jaegere, Department of Cardiology, Erasmus Medical Center, PB 412, 3000 CA Rotterdam, the Netherlands. E-mail: p.dejaegere@erasmusmc.nl.

REFERENCES

1. Piazza N, Grube E, Gerckens U, et al. Procedural and 30-day outcomes following transcatheter aortic valve implantation using the third generation (18 Fr) CoreValve ReValving system. EuroIntervention 2008;4:242–9.
2. Thubrikar M, Piepgrass WC, Shaner TW, Nolan SP. The design of the normal aortic valve. Am J Physiol 1981;241:H795–801.
3. Tops LF, Wood DA, Delgado V, et al. Noninvasive evaluation of the aortic root with multislice computed tomography: implications for transcatheter aortic valve replacement. J Am Coll Cardiol Img 2008;1:321–30.
4. Piazza N, de Jaegere P, Schultz C, Becker P, Serruys PWJS, Anderson R. Anatomy of the aortic valvar complex and its implications for transcatheter implantation of the aortic valve. Circ Cardiovasc Intervent 2008;1:74–81.
5. Walsh CR, Larson MG, Kupka M, et al. Association of aortic valve calcium detected by electron beam computed tomography with echocardiographic aortic valve disease and with calcium deposits in the coronary arteries and thoracic aorta. Am J Cardiol 2004;93:421–5.
6. Zegdi R, Ciobotaru V, Noghin M, et al. Is it reasonable to treat all calcified stenotic aortic valves with a valved stent? Results from a human anatomic study in adults. J Am Coll Cardiol 2008;51:579–84.
7. Weustink AC, Meijboom WB, Mollet NR, et al. Reliable high-speed coronary computed tomography in symptomatic patients. J Am Coll Cardiol 2007;50:786–94.
8. Piazza N, Onuma Y, Jesserun E, et al. Early and persistent intraventricular conduction abnormalities and requirements for pacemaking after percutaneous replacement of the aortic valve. J Am Coll Cardiol Intv 2008;1:310–6.
9. Cribier A, Eltchaninoff H, Bash A, et al. Percutaneous transcatheter implantation of an aortic valve prosthesis for calcific aortic stenosis: first human description. Circulation 2002;106:3006–8.
10. Otto CM. Valvular aortic stenosis: disease severity and timing of intervention. J Am Coll Cardiol 2006;47:2141–51.
11. Kulik A, Burwash IG, Kapila V, Mesana TG, Ruel M. Long-term outcomes after valve replacement for low-gradient aortic stenosis: impact of prosthesis-patient mismatch. Circulation 2006;114 Suppl:I553–8.
12. Lüscher TF, Steffel J, Eberli FR, et al. Drug-eluting stent and coronary thrombosis: biological mechanisms and clinical implications. Circulation 2007;115:1051–8.
13. Schultz C, Piazza N, Weustink A, et al. Valve in valve percutaneous aortic prosthesis for acute regurgitation is not a benign procedure: an analysis of Corevalve geometry using MSCT and IVUS. Eurointervention 2009. In press.

Key Words: cardiac computed tomography ■ percutaneous valve replacement ■ aortic valve.